Calcium and Cell Cycle Progression: Possible Effects of External Perturbations on Cell Proliferation

Irina Baran
Biophysics Laboratory, Biotehnos S.A., Dumbrava Rosie 18, Bucharest 70254, Romania

ABSTRACT Exit from the phase of cellular division appears to be driven by a calcium signal that triggers a cascade of events leading to the completion of mitosis. Here we propose a model that relates the dynamics of cytosolic calcium to progression through mitosis, G_1 and G_2 phases of the cell cycle. To this end, the assumption has been made that the transient rise in cytosolic calcium concentration during mitosis is induced by inositol(1,4,5)triphosphate (IP_3), which in turn is released at high levels of mitosis-promoting factor (MPF). On this basis, a system of ordinary differential equations is proposed to simulate the evolution of ten cell-cycle-specific molecular species, including cyclins A and B, MPF, IP_3, Ca^{2+}, the $CaMK_{II}$ holoenzyme, and the ubiquitination complex. The influence on the cell proliferation capacity exerted by external perturbations, like calcium microinjections, depletion of intracellular calcium stores, electromagnetic fields, or stimulation/inhibition of different calcium currents through the plasma membrane, can be studied by appropriate modulation of the parameters involved in the signal transduction pathway.

INTRODUCTION

In dividing cells the phase of cellular division (mitosis) is marked at anaphase by significant changes in cytosolic calcium concentration, which are much more strongly expressed in embryos than in somatic cells (Alberts et al., 1989; Whitaker, 1993). Although the molecular mechanisms that lead to the increase of calcium in cytosol at anaphase are not yet understood, there is evidence (Clapa et al., 1994) that in early sea urchin embryos the mitotic calcium transients are due to an endogenous mechanism of releasing Ca^{2+} from internal calcium stores via an increase of inositol(1,4,5)triphosphate (IP_3). In addition, the well-known features of the IP_3-induced calcium release make it a good candidate for relating MPF (mitosis-promoting factor) activation with the mitotic calcium increase. Likewise, it appears natural to consider that the release of calcium from internal stores, like the endoplasmic reticulum (ER), is an important step in the cascade of mitotic events. So far, stress has been placed on the way mitosis is triggered, as derivation of the molecular steps involved has been facilitated by genetic and biochemical studies (Gould and Nurse, 1989; McIntosh and Koonce, 1989; Murray, 1992; Murray and Kirschner, 1989; O'Farrell et al., 1989; Nurse, 1990). Instead, exit from mitosis, with its decisional moment placed in anaphase, seems to be connected to a sudden increase in cytosolic calcium (Alberts et al., 1989; Whitaker, 1993) and to the appearance of a force generating chromosome movements on the spindle (Li and Nicklas, 1995; Murray, 1995). We think an intrinsic relationship between these two elements exists that is similar to the calcium-dependent process of generating force in muscle cells. Indeed, it is known (McIntosh and Koonce, 1989) that injection of calcium causes spindle dissolution and anaphase onset, and injected antibodies against Ca^{2+} transport proteins cause spindle dissolution as well. Therefore, it might be of real interest to predict the dynamics of calcium and other mitosis-related molecular species, to follow the influence of external signals upon cellular division.

The IP_3-induced calcium release from internal stores in response to external stimuli is known (Finch et al., 1991; Iino and Endo, 1992; Berridge, 1993; Camacho and Lechleiter, 1993) as a basic element in the signal pathway that leads to the oscillating behavior of calcium. New insights into the mechanisms underlying the cytosolic calcium oscillations have been gained through theoretical considerations of the involvement of IP_3 in generating periodic calcium spikes (Chay, 1993; Eichwald and Kaiser, 1993). Furthermore, IP_3 appears to be the main factor that underlies the Ca^{2+} oscillations, and the presence of high-sensitivity IP_3 receptors at the primary sites of initiation of Ca^{2+} spikes was demonstrated in experiments with agonists (Kasai et al., 1993; Thorn et al., 1993). Although the external messenger-induced production of IP_3, which diffuses intracellularly from the membrane, seems as well to be supported by results on *Xenopus* or hamster eggs after fertilization (Clapa et al., 1994; Miyazaki et al., 1992), the question is raised of how somatic cells achieve the increase in cytosolic calcium in anaphase without the action of an external stimulus. It has been shown (Clapa et al., 1994) that in early sea urchin embryos, which have sharply synchronized divisions, an endogenous mechanism of inducing IP_3 oscillations in the cell cycle exists, which seems to be independent of the cyclin oscillator. Instead, somatic cells are characterized by the variability of the cell cycle timing, which is mainly due to the G_1 phase regulation. Therefore the hypothesis of two uncoupled, IP_3 and mitotic cyclin (cyclin B) oscillators is not to be applied here, because the risk of overlapping the

Received for publication 13 June 1995 and in final form 17 November 1995.

Address reprint requests to Dr. Irina Baran, Biophysics Laboratory, Biotehnos S.A., Dumbrava Rosie 18, Bucharest 70254 Romania. Tel.: 00401-685-7224; Fax: 00401-210-9705; E-mail: baran@roifa.ifa.ro.

0006-3495/96/03/1198/16 $2.00

MPF activation with the calcium signal would be very high, leading to an improper division. This aspect has been considered earlier (Baran, 1994a) but remains a fundamental assumption of the study we present here. In the absence of conclusive observations in this matter, we can only speculate that there is indeed a succession of events that relate active MPF to IP_3 production in a cause-effect relation. A more detailed description of the hypothesis proposed in this kind of approach has been given elsewhere (Baran, 1994a). In that model, from which this study has followed, a scheme involving eight molecular species was proposed to describe the fundamental biochemical changes a cell experiences during division. There, the eight internal parameters were chosen as follows: four distinct forms of the (mitotic) cyclin B · $p34^{cdc2}$ complex, IP_3, cytosolic Ca^{2+}, the calmodulin-dependent kinase ($CaMK_{II}$) holoenzyme, and the ubiquitination complex. Although the model gave a satisfactory description of their evolution during cell division, it was restricted to progression through G_2 and mitosis and thus was unable to provide any connection to the remainder of the cell cycle.

Earlier theoretical models of the cell cycle (Norel and Agur, 1991; Thron, 1991, 1994) took into consideration a small number of nonlinear ordinary differential equations, based on the most general features of MPF and mitotic cyclin. Yet, a detailed and accurate analysis of the molecular mechanisms involved in the normal cell cycle progression is needed if one seeks realistic quantitative results regarding the variety of cellular events between two successive divisions. Recently, consistent theoretical models proposed by Novak and Tyson (1993, 1995) provided new criteria for characterizing the mitotic control apparatus and the coordination between growth and division.

The purpose of the present work is twofold. First, this study is aimed at discussing a model that allows the characterization of the cell status throughout the cell cycle, in a dynamical approach. More precisely, we express the major molecular interactions that take place in a cell during the cell cycle progression, in ten differential equations that yield the evolution of specific cellular quantities. The model proposed here adds major improvements to the prior model (Baran, 1994a), in the sense that it considers a more complete picture of the processes governing calcium dynamics, and adapts the equations to the entire division cycle. Consequently, it admits a cell-cycle-specific oscillatory solution. Second, it attempts to provide a possibility of quantitating the effects of different external stimuli upon cellular division, by following the changes induced in the behavior of several specific intracellular parameters.

To this end we shall not stress a number of equations that were presented elsewhere (Baran, 1994a). However, some relevant aspects emerge from adding new elements with regard to dynamics of calcium concentration in internal stores, the regulation of the mitotic cyclin synthesis, or the mitosis-specific cellular response to external fields. In this sense the equation that yields the evolution of the cyclin B · $p34^{cdc2}$ inactive complex had to be modified, to contain the term of production that is known to take place before mitosis. To consider a realistic form of this term, we take into account the restriction that forces the mitotic cyclin to accumulate not earlier than the S phase (Amon et al., 1994; Seufert et al., 1995). This refers to the rapid proteolysis mitotic cyclin is subjected to in G_1, thus failing to accumulate despite its nonzero synthesis rate. Likewise, in agreement with these experimental observations, previous results (Baran, 1994a) suggested the ubiquitination complex that is produced in late mitosis to degrade the mitotic cyclin is still present after the disappearance of the cyclin B · $p34^{cdc2}$ active complex. On this basis the model we propose here will reconsider the quantitative relation between both the accumulation and destruction of cyclin B and the ubiquitination complex, which should be not confined to a short period at the end of M phase.

Finally, it is worth saying that involvement of IP_3 in inducing mitotic calcium transients gains increasing ground (Miyazaki et al., 1992; Clapa et al., 1994), as does the feedback loop between cytosolic calcium and the IP_3 production pathway, which leads to IP_3-induced calcium release from intracellular stores (Finch et al., 1991; Iino and Endo, 1992). Theoretical considerations of this mechanism (Eichwald and Kaiser, 1993) have demonstrated that this positive feedback can induce self-sustained oscillations of intracellular calcium, thus accounting for the stability against noise and high sensitivity to periodic perturbations, features that are specific to the nonlinear oscillators.

Relying on these considerations, we found it useful to investigate the possible effects of external factors on mitosis-specific intracellular dynamics, as recent fura-2 techniques of calcium measurements enable fast determination of the cellular calcium metabolism interaction with, for example, electromagnetic fields. In particular, the model can be extended to follow calcium-mediated apoptosis in cancerous cells exposed to ionizing radiation, because there is evidence for large (even lethal) increases in cytosolic calcium after irradiation of transformed cells.

However, we should emphasize that involvement of calcium in cell cycle progression remains an open problem regarding its role at different points in the cell cycle, particularly at anaphase. Meanwhile, the experimental data in this area are still few, so further investigations are needed to clarify and settle the molecular mechanisms involved. For instance, a direct role of calcium in mitogenesis of somatic cells has been revealed (Pardee, 1989; Dubois and Rouzaire-Dubois, 1993) in which IP_3 is also involved, whereas for mitosis the only conclusive observations were obtained on eggs or early embryos. Our model assumes the same sequence of calcium-related events as proposed (Whitaker, 1993) for embryos.

MODEL FOR CELL CYCLE PROGRESSION

The processes involved in cell cycle progression have been intensively studied (Félix et al., 1992; Glotzer et al., 1991;

Gould and Nurse, 1989; Hartwell, 1974; Hartwell and Weinert, 1989; Hunt, 1992; Lorca et al., 1993; McIntosh and Koonce, 1989; Moreno and Nurse, 1994; Murray and Kirschner, 1991; O'Farrel et al., 1989; Pardee, 1989; Parker and Piwnica-Worms, 1992; Wu and Russell, 1993; Yamashiro et al., 1991). For this reason we do not expand on the meaning of the variables we use in the remainder of the work or on the derivation of several equations, which were described within other models (Baran, 1994a,b; Eichwald and Kaiser, 1993). The model here proposed matches the wild-type yeast cell cycle, but universality of the processes involved allows the extension to different eukaryotic cells. Three basic hypotheses are assumed in the model, namely that in somatic cells: i) IP_3 is released during mitosis, consequently to the endogenous activation of MPF; ii) IP_3 is the main factor responsible for the calcium release in cytosol; and iii) the mitotic calcium transient sets in motion the cyclin B degradation machinery, as in the corresponding scenario in embryos.

Let CB denote the complex of cyclin B bound to phosphorylated $p34^{cdc2}$ (phosphorylation sites are the tyrosine 15 and threonine 16 residues of $p34^{cdc2}$ in fission yeast), which subsequently is dephosphorylated at tyrosine 15 and thus generates the appearance of pre-MPF, that is the cyclin B · $p34^{cdc2}$ inactive conjugate, noted preMPF. Next, activation of the protein kinase activity of $p34^{cdc2}$ and cyclin phosphorylation give rise to MPF (MPF). This induces the release of IP_3 at a rate considered here to depend both on the MPF and cytosolic Ca^{2+} concentration ($[Ca^{2+}]_i$), accounting for the positive feedback loop between cytosolic calcium and the IP_3 production pathway. The IP_3-induced release of calcium from internal stores into the cytosol is followed by refilling of the stores through the action of a calcium pump. The calcium content in cytosol ($[Ca^{2+}]_i$) and that in intracellular stores ($[Ca^{2+}]_s$) vary with time according to the equations proposed in a model for receptor-controlled cytosolic calcium oscillations (Eichwald and Kaiser, 1993), where the dynamics of IP_3 results from activation mechanisms different of those considered in the present study.

Investigations on anaphase triggering and exit from mitosis have led to the conclusion that the calcium-dependent signal that determines the initiation of chromosome movement to the poles follows a calmodulin-specific pathway on which the calmodulin-dependent kinase $CaMK_{II}$ is activated (Lorca et al., 1993; Whitaker, 1993). This in turn induces (Whitaker, 1993) the production of the ubiquitination complex (UbC) that conjugates to cyclin B, which in this way becomes extremely sensitive to degradation (Glotzer et al., 1991; Seufert et al., 1995) and is rapidly destroyed. This fact involves the inactivation of MPF, through the intermediate product ubiquitinated cyclin B · $p34^{cdc2}$ (denoted UbMPF), and marks the end of mitosis through telophase. Absence of active $p34^{cdc2}$ kinase and cyclin B is followed by synthesis of G_1 cyclins, here denoted generically cyclin A, which binds to $p34^{cdc2}$ in the G_1 phase of the cell cycle. The complex formed, cyclin A · $p34^{cdc2}$ (CA), is negatively regulated by cyclin B, which begins to accumulate in late S–G_2, and therefore the CA level decays before mitosis. A picture of these events is schematically represented in Fig. 1.

The appearance of CB in doubly phosphorylated form follows from a succession of molecular events that was finely analyzed by Novak and Tyson (1993, 1995) in their models, where kinetics of cyclin B and that of the distinct forms of $p34^{cdc2}$ are considered in separate equations.

Disappearance of CB is due to a sequence of events that culminates with MPF genesis. The control mechanisms that operate on this part of the cell cycle include the stimulating and, respectively, inhibitory action of the *cdc*25 and *wee*1 genes upon dephosphorylation of $p34^{cdc2}$. For this reason, the step

$$\mathrm{CB} \rightleftharpoons \mathrm{preMPF} \tag{1}$$

was assumed (Baran, 1994a,b) to be an enzymatic process with noncompetitive inhibition (see Appendix). The autocatalytic activation of MPF, which is assumed to be achieved through a step of the form

$$\mathrm{preMPF} + \mathrm{MPF} \rightarrow 2\mathrm{MPF} \tag{2}$$

is enhanced (Baran 1994a) by a one-step enzymatic reaction

$$\mathrm{preMPF} \rightleftharpoons \mathrm{MPF} \tag{3}$$

with Michaelis-Menten kinetics. Finally, MPF stimulates directly the dephosphorylation of CB, and the evolution of [CB] and [preMPF] is given then by the following equations:

$$\frac{d[CB]}{dt} = \frac{s_1 \cdot [CB]}{K_{1s} + [CB]} e^{-\gamma_8[UbC]} e^{-\gamma_3[MPF]} - h_1[CB] - (1 - e^{-\gamma_1[CB]}) \frac{k_1 \cdot [CB]}{K_{1M} + K_1[CB]} \cdot \frac{k_3 \cdot [MPF]}{K_{3M} + [MPF]} \tag{4}$$

and, respectively,

$$\frac{d[preMPF]}{dt} = (1 - e^{-\gamma_1[CB]}) \frac{k_1 \cdot [CB]}{K_{1M} + K_1[CB]} \cdot \frac{k_3 \cdot [MPF]}{K_{3M} + [MPF]} - \frac{k_2 \cdot [preMPF]}{K_{2M} + [preMPF]} (1 + k \cdot [preMPF] \cdot [MPF]), \tag{5}$$

where k is the rate constant of the reaction in Eq. 2. The rate of CB production is modeled by the first term in the right side of Eq. 4, assumed to have Michaelis-Menten kinetics. However, the use of a constant production term s_1 instead of a sigmoidal dependence as chosen ($s_1[CB]/(K_{1s} + [CB])$) does not change significantly the oscillatory solution of the system. The constraints that prevent cyclin B from accumulating as long as the ubiquitination complex and MPF are active are introduced in the model through the exponential terms that multiply the term $s_1[CB]/(K_{1s} + [CB])$. The use of these terms in exponential form guarantees the inhibition of cyclin B synthesis at high levels of MPF and UbC.

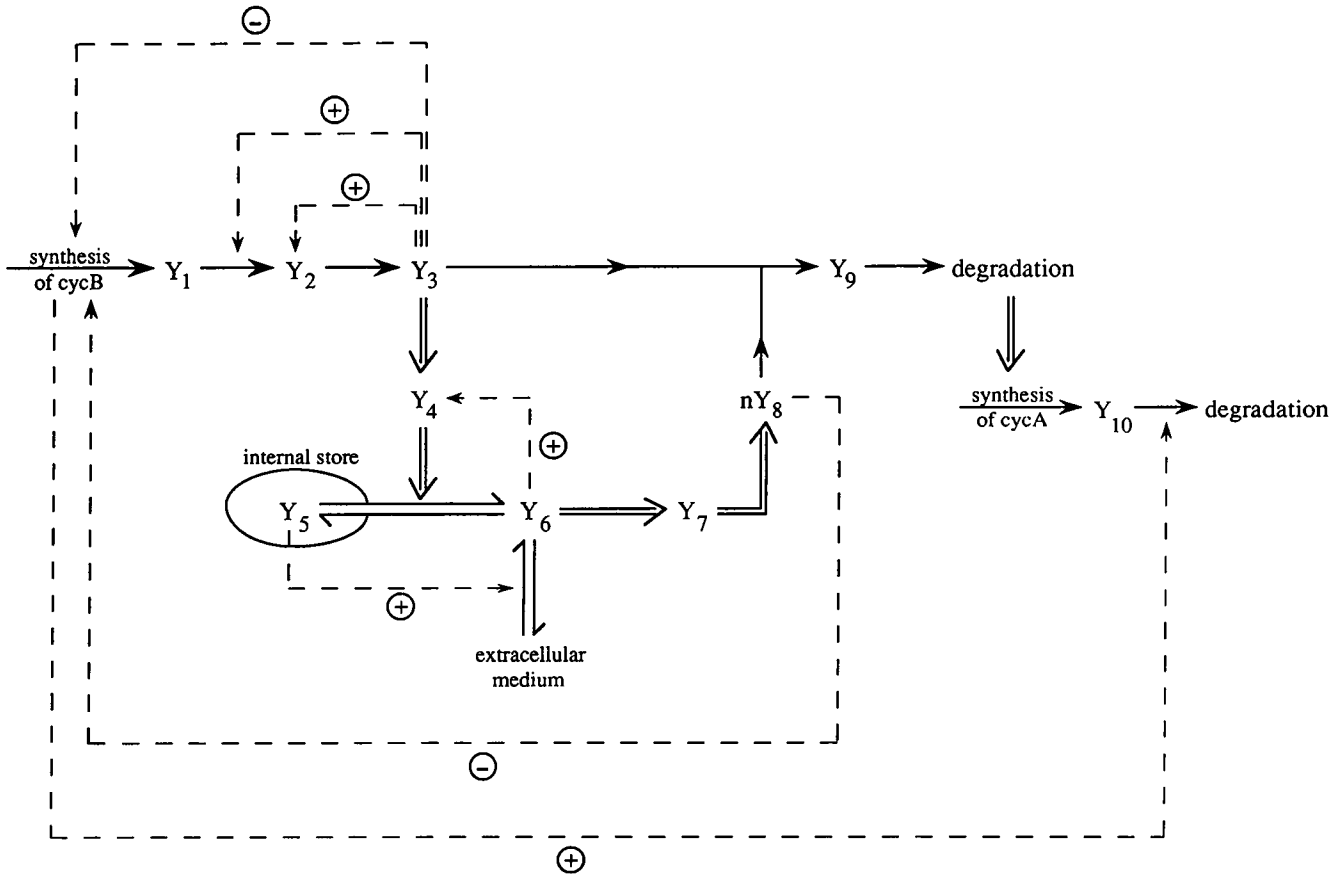

FIGURE 1 The flow of cell cycle events as considered in the model. Y_i ($i = 1, \ldots, 10$) represent CB (Y_1), preMPF (Y_2), MPF (Y_3), IP_3 (Y_4), $[Ca^{2+}]_s$ (Y_5), $[Ca^{2+}]_i$ (Y_6), $CaMK_{II}$ (Y_7), UbC (Y_8), UbMPF (Y_9), and CA (Y_{10}), respectively. The positive (+) and negative (−) feedback loops are represented by dashed arrow lines. Solid arrow lines give biochemical reactions in which the molecular species Y_i involved are either reacting or produced. The implication of several Y_i in triggering the subsequent biochemical step is marked by a double arrow. Finally, $\rightleftharpoons$ depicts the calcium interchanges between cytosol and internal stores/extracellular medium.

Because the mechanisms underlying the respective inhibitory actions are not clear, the choice of the mathematical form is of course economic but follows the logic in the modeling approach. However, it is worth mentioning that considering a more appropriate dependence, on the basis of a chemically inhibitory form, would clearly improve the model and yield a more realistic solution. Dissociation of the cyclin B · $p34^{cdc2}$ complex is given in Eq. 4 by the negative linear term $(-h_1[CB])$, whose rate constant h_1 is assumed to be constant throughout the cell cycle, as in the case of *Xenopus* (Kobayashi et al., 1994). The possibility of obtaining the h_1 value by experiment is clearly a gained point. Indeed, the procedure (Kobayashi et al., 1994) that yields the half-time of dissociation of cyclin B (and A) from $p34^{cdc2}$ is now available. Therefore h_1 can be obtained by a simple calculus as

$$h_1 = \frac{\ln 2}{t_{1/2}^{B}}, \tag{6}$$

where $t_{1/2}^{B}$ is the cyclin B · $p34^{cdc2}$ dissociation half-time determined in experiments. Here we assume that dissociation of cyclin B from $p34^{cdc2}$ is negligible for two other forms of the complex cyclin B · $p34^{cdc2}$, namely preMPF and MPF, as preMPF is rapidly transformed in the active form MPF, and MPF is inactivated under the action of the ubiquitination complex. Finally, the component $(1 - \exp(-\gamma_1[CB]))$ appearing in Eqs. 4 and 5 is the main factor responsible for the delay of the MPF activation until the maximum level of CB is reached.

In the model, the rate of IP_3 release in mitosis depends on the MPF level and on the concentration of calcium in cytosol. Taking into account the positive feedback of cytosolic Ca^{2+}, we assume as proposed (Baran, 1994a) that a simple form of the IP_3 dynamics equation able to reproduce its highly nonlinear character at anaphase is

$$\frac{d[IP_3]}{dt} = \frac{k_{34} \cdot [MPF]^4}{K_3^4 + [MPF]^4} \cdot \frac{[Ca^{2+}]_i^2}{K_6^2 + [Ca^{2+}]_i^2} - h_4 \cdot [IP_3], \tag{7}$$

where the last term on the right side is related to the disappearance of IP_3 but may also include other mechanisms operating in mitosis.

The equations proposed (Eichwald and Kaiser, 1993) to govern the evolution of calcium concentration in cytosol and internal stores read as follows:

$$\frac{d[Ca^{2+}]_s}{dt} = \beta([Ca^{2+}]_i) - \rho([IP_3], [Ca^{2+}]_s) - k_5[Ca^{2+}]_s, \tag{8}$$

where the term

$$\beta([Ca^{2+}]_i) = \frac{k_{56}[Ca^{2+}]_i^r}{K_P^r + [Ca^{2+}]_i^r} \tag{9}$$

describes the influx of calcium into the store due to the ATP-driven calcium pump. The next term,

$$\rho([IP_3], [Ca^{2+}]_s) = \frac{k_{54}[IP_3]^m}{(K_R + [IP_3])^m}[Ca^{2+}]_s, \tag{10}$$

represents the rate of the IP_3-induced release of calcium in cytosol. The exponent m characterizes the degree of cooperativity in the opening of the channels by IP_3. Finally, the linear term on the right side of Eq. 8 describes a passive flux of calcium out of the store, with rate constant k_5. This flux is determined by the difference in the calcium concentration of the two zones, as the calcium concentration is much higher inside the store. We should point out that the difference between cytosol and the extracellular region is of about the same magnitude.

The dynamics of cytosolic calcium is the result of the balance of the calcium interchanges between stores and cytosol and, respectively, between cytosol and the extracellular medium. The following equation then is used:

$$\frac{d[Ca^{2+}]_i}{dt} = -\beta([Ca^{2+}]_i) + \rho([IP_3], [Ca^{2+}]_s) + k_5[Ca^{2+}]_s + \alpha([IP_3]) + \phi([Ca^{2+}]_s) + s_6 - k_6 \cdot [Ca^{2+}]_i. \tag{11}$$

The steady (s_6) and linear ($k_6 \cdot [Ca^{2+}]_i$) terms are proposed to model the passive influx of calcium from the outside and, respectively, the activity of pumping Ca^{2+} out of cytoplasm by pumps on the plasma membrane. During mitosis, part of free Ca^{2+} can bind to specific proteins (like calmodulin). We assume the rate of binding to be included in the term $k_6 \cdot [Ca^{2+}]_i$ and hence that the activity of pumps on the plasma membrane to be consequently diminished. When the extracellular medium contains no Ca^{2+}, $s_6 = 0$. In addition, depletion of intracellular calcium stores, induced by, for example, ionomycin or excess of EGTA, activates a calcium inward current (Parekh et al., 1993; Randriamampita and Tsien, 1993) through an unknown mechanism which has been proposed, contradictorily, to be either caused by (Luckhoff and Clapham, 1992) or, respectively, independent of (Hoth and Penner, 1992) IP_3 or IP_4. In this sense, the influx of extracellular calcium described by the term

$$\alpha([IP_3]) = \frac{k_{64}[IP_3]^q}{(K_M + [IP_3])^q} \tag{12}$$

is correlated (Eichwald and Kaiser, 1993) to the opening of calcium channels in the plasma membrane that may be caused by IP_3 or by a IP_3 derivate. Furthermore, we have introduced an additional flux,

$$\phi([Ca^{2+}]_s) = \phi_0 - \phi_1[Ca^{2+}]_s, \tag{13}$$

to account for the IP_3-independent mechanism that monitors the calcium content of the ER and relates it to a sustained, capacitive influx of Ca^{2+} (Hoth and Penner, 1992). For simplicity we consider a linear dependence of this current on the content of calcium stores. Our investigations showed that introducing ϕ in Eq. 11 leads to stabilization of the basal level of stores outside mitosis. A schematic depiction of the different calcium fluxes and related events during mitosis is given in Fig. 2.

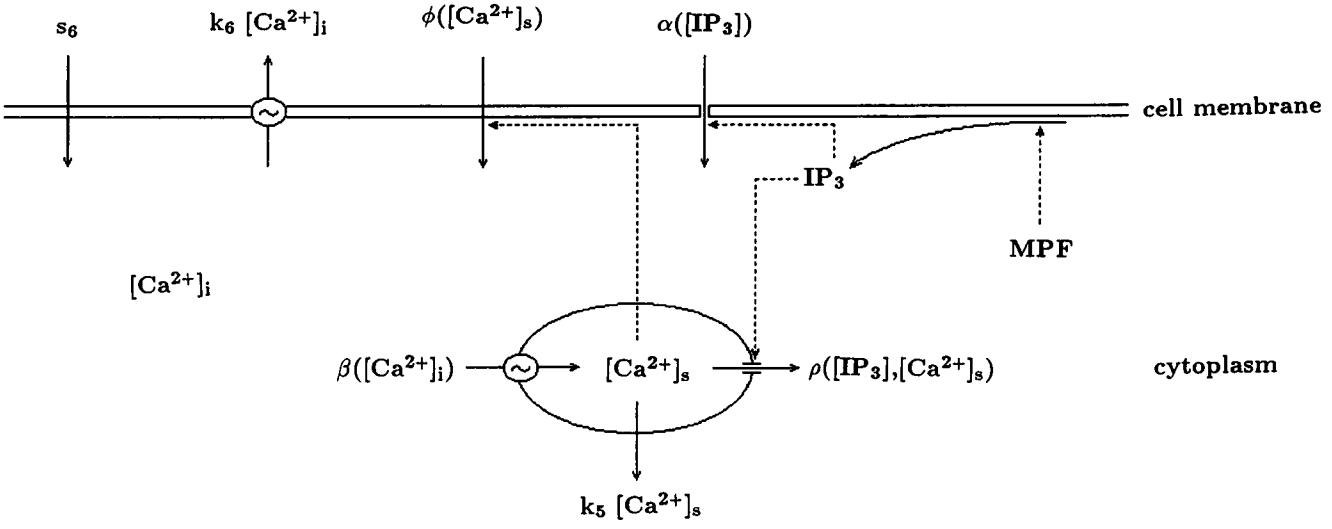

FIGURE 2 Calcium-related events during cell division, as considered in the model. The different calcium fluxes are indicated by notations used in text. The IP_3 production generated by MPF leads to the calcium increase, which induces the inactivation of MPF through a $CaMK_{II}$-dependent pathway.

The excess of calcium in cytosol leads to the activation of the $CaMK_{II}$ holoenzyme at a rate given by the equation as proposed (Baran, 1994a):

$$\frac{d[CaMK_{II}]}{dt} = \frac{k_{67} \cdot ([Ca^{2+}]_i - [Ca^{2+}]_{i,0})^3}{K_{6M}^3 + ([Ca^{2+}]_i - [Ca^{2+}]_{i,0})^3} - k_7 \cdot [CaMK_{II}] + s_7, \quad (14)$$

where $[Ca^{2+}]_{i,0}$ is the basal level of cytosolic calcium. The ubiquitination complex then is produced at a rate that is considered to be given by a linear $[CaMK_{II}]$-dependent term, so that we obtain the equation

$$\frac{d[UbC]}{dt} = k_8 \cdot [CaMK_{II}] - \frac{k_{38}}{n} \cdot [MPF] \cdot [UbC]^n - h_8 \cdot [UbC]. \quad (15)$$

The second term of the right side derives easily from the kinetics of cyclin B multiubiquitination at a single site (Glotzer et al., 1991):

$$MPF + n[UbC] \rightarrow UbMPF, \quad (16)$$

where k_{38} is the first-order rate constant and n represents the degree of cyclin B ubiquitination.

Finally, the evolution of MPF in mitosis is obtained as

$$\frac{d[MPF]}{dt} = \frac{k_2 \cdot [preMPF]}{K_{2M} + [preMPF]}(1 + k \cdot [preMPF] \cdot [MPF]) - \frac{k_3 \cdot [MPF]}{K_{3M} + [MPF]} - k_{38} \cdot [MPF] \cdot [UbC]^n - h_3 \cdot [MPF], \quad (17)$$

where the last term takes into account the loss through other enzymatic pathways. According to Eq. 16 we suppose that the variation of the UbMPF level obeys the equation

$$\frac{d[UbMPF]}{dt} = k_{38} \cdot [MPF] \cdot [UbC]^n - h_9 \cdot [UbMPF], \quad (18)$$

where the coefficient h_9 determines the rate of UbMPF degradation.

Cyclin A begins to accumulate after UbMPF disappearance and binds to $p34^{cdc2}$. A simple form is considered for the equation governing the dynamics of the complex formed (CA):

$$\frac{d[CA]}{dt} = s_{10} e^{-\eta_9 [UbMPF]} e^{-\eta_1 [CB]} - h_{10} \cdot [CA], \quad (19)$$

where s_{10} (= const.) is the maximum rate of CA appearance, assumed to be reached in G_1, when [CB] = [UbMPF] = 0. The persistence of the ubiquitination complex after mitosis (when [UbMPF] = 0) prevents cyclin B accumulation, which in turn allows [CA] to rise. This consideration is based on the experimental evidence that mitotic cyclins repress the expression of G_1 cyclins (Amon et al., 1994). For these reasons we have multiplied s_{10} by the two exponential terms. The last term in Eq. 19 gives the rate of cyclin A · $p34^{cdc2}$ dissociation with rate constant h_{10}, which has been shown to be constant over the cell cycle (Kobayashi et al., 1994). Similarly, with Eq. 6 we have again

$$h_{10} = \frac{\ln 2}{t_{1/2}^A}, \quad (20)$$

where $t_{1/2}^A$ is the cyclin A dissociation half-time, which can be obtained by experiment. However, the role of G_1 cyclins in commitment to the S phase needs to be clearly understood, so that a comprehensive model of the S phase onset could be obtained. Because the rate of cyclin A · $p34^{cdc2}$ production follows the variation of cyclin A concentration (the level of $p34^{cdc2}$ is constant over the division cycle), accessing cyclin A kinetics would greatly improve Eq. 19. Likewise, a possible extension of the model to higher eukaryotes should make a clear distinction between the different roles and timing of cyclins A, C, D, and E in progression through the G_1 and S phases (Elledge et al., 1992; Knoblich et al., 1994; Walker and Maller, 1991).

A final point should be discussed here: the number of equations used in the model is quite large (ten), and thus may seem inconvenient for numerical simulations. But this situation is to be preferred, as all the molecular events considered are of fundamental importance in cell progression toward division. If the normal evolution of a single state variable is significantly perturbed, the cell stops on its way to division and triggers specific cellular mechanisms to remove the perturbation effects. Furthermore, one may say that the number of ten cellular parameters as chosen in the model is rather scant for our goals, and the supplementary parameters of a more complete modeling system would help fulfill the major requirements implied by experimental observations.

NUMERICAL SIMULATION OF NORMAL MITOSIS

The highly nonlinear structure of the dynamical system consisting of Eqs. 4–5, 7, 11, 14–15, and 17–19 does not allow us to find an analytical solution. Therefore, we solved the dynamical system by the fourth-order Runge-Kutta method, with a time step of 0.001 units. Rather than stressing the precise determination of the cellular parameters, we wanted to find out whether the system can simulate the succession of cell cycle events on the basis of the interactions depicted in Fig. 1. To this end we have studied the optimal setting of the parameters that could fit the wild-type yeast cell cycle, whose duration varies with the temperature and the yeast type. Thus, the fission yeast *Schizosaccharomyces pombe* completes one cycle in 180 min at 29°C (Mitchison, 1989, cited in Novak and Tyson, 1995) and the budding yeast *Saccharomyces cerevisiae* takes around 100 min at 30°C (Hartwell, 1974) to grow and divide. The mechanisms involved in cell cycle progression are similar in fission and budding yeast and we took as a reference the values obtained in experiments with *S. cerevisiae*: the doubling time of cells grown in YPD medium at 30°C may be

(Slater, 1977) 85 min for large cells (fast growth) or 104 min for small cells (slow growth). In both cases the S, G_2, and M phases are completed in the same time, whereas G_1 duration varies. The data of John (1981) show that cells grown at 30°C complete a division cycle in 132 min. Here we consider a generic duration of the cell cycle of 120 min. We adjusted the parameter values to obtain an oscillatory solution of period 120 min, with nuclear division (discussed below) comprised in a time fraction as large as 0.19 of the cell cycle. The following constant parameters have been used: $s_1 = 4000$ nM/min; $K_{1s} = 760$ nM; $\gamma_8 = 3$ nM^{-1}; $\gamma_3 = 10^{-3}$ nM^{-1}; $h_1 = 2.5$ min^{-1}; $\gamma_1 = 5 \cdot 10^{-3}$ nM^{-1}; $k_1 = 162.55$; $K_{1M} = 150$ nM; $K_1 = 30$; $k_2 = 50$ nM/min; $K_{2M} = 20$ nM; $k_3 = 60$ nM/min; $K_{3M} = 300$ nM; $k = 5$ nM^{-2}; $k_{34} = 700$ nM/min; $K_3 = 300$ nM; $h_4 = 1$ nM^{-1}; $k_{56} = 550$ nM/min; $k_{54} = 50$ nM/min; $K_R = 650$ nM; $k_{64} = 20$ nM/min; $K_M = 100$ nM; $\phi_0 = 120$ nM/min; $\phi_1 = 0.04$ min^{-1}; $s_6 = 10$ nM/min; $k_{67} = 800$ nM/min; $k_7 = 2.1$ min^{-1}; $s_7 = 1$ nM/min; $k_8 = 30^{-1}$ min^{-1}; $n = 3$; $k_{38} = 0.06$ nM^{-3} min^{-1}; $h_8 = 0.5$ min^{-1}; $h_3 = 0.008$ min^{-1}; $h_9 = 2.5$ min^{-1}; $s_{10} = 580$ nM/min; $\eta_9 = 0.5$ nM^{-1}; $\eta_1 = 0.2$ nM^{-1}; $h_{10} = 5$ min^{-1}.

In the present study we suppose that the interphasic dynamics of the cytosolic Ca^{2+} resumes to a quasi-steady state determined by the basal concentration $[Ca^{2+}]_{i,0} = 200$ nM, while the concentration of Ca^{2+} inside the stores reaches the level $[Ca^{2+}]_{s,0} = 3000$ nM, and $[IP_3] = 0$. On this basis we can choose appropriate parameter values that obey the equalities $k_5 = \beta([Ca^{2+}]_{i,0})/[Ca^{2+}]_{s,0}$ and $k_6 = s_6/[Ca^{2+}]_{i,0}$ derived from the conditions that $d[Ca^{2+}]_s/dt = d[Ca^{2+}]_i/dt = 0$ and $[IP_3] = 0$. So, $k_5 = 11/600$ min^{-1} and $k_6 = 0.05$ min^{-1}.

The value of the Michaelis-Menten constant of the calcium pump of the internal store is set to $K_P = 600$ nM, because $[Ca^{2+}]_i$ can reach values greater than 1000 nM, whereas the values $r = 2$ and $m = 4$ are fixed as in the paper of Eichwald and Kaiser (1993), considering that the number of ions transported by the calcium pump is two and assuming cooperativity in the opening of calcium channels by IP_3.

Limit cycle oscillations are obtained (as shown in Figs. 3 and 4) in good agreement with the temporal order of the cell cycle events and with the highly nonlinear character of the dynamics of the molecular species considered within the model. Stability of the oscillations persists within wide

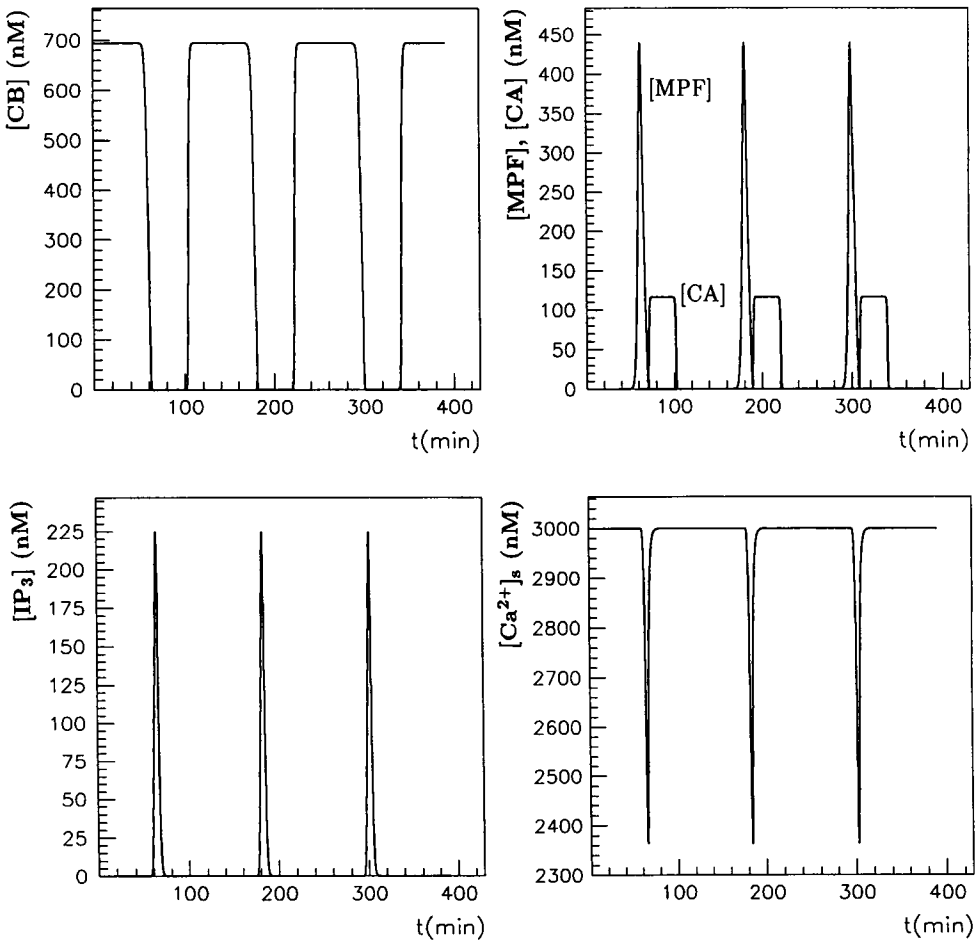

FIGURE 3 Time evolution of the concentrations of the cyclin B · p34^{cdc2} inactive complex ([CB]), MPF, cyclin A · p34^{cdc2} complex ([CA]), IP_3, and the calcium content of internal stores ($[Ca^{2+}]s$) given by the solution of the dynamical system.

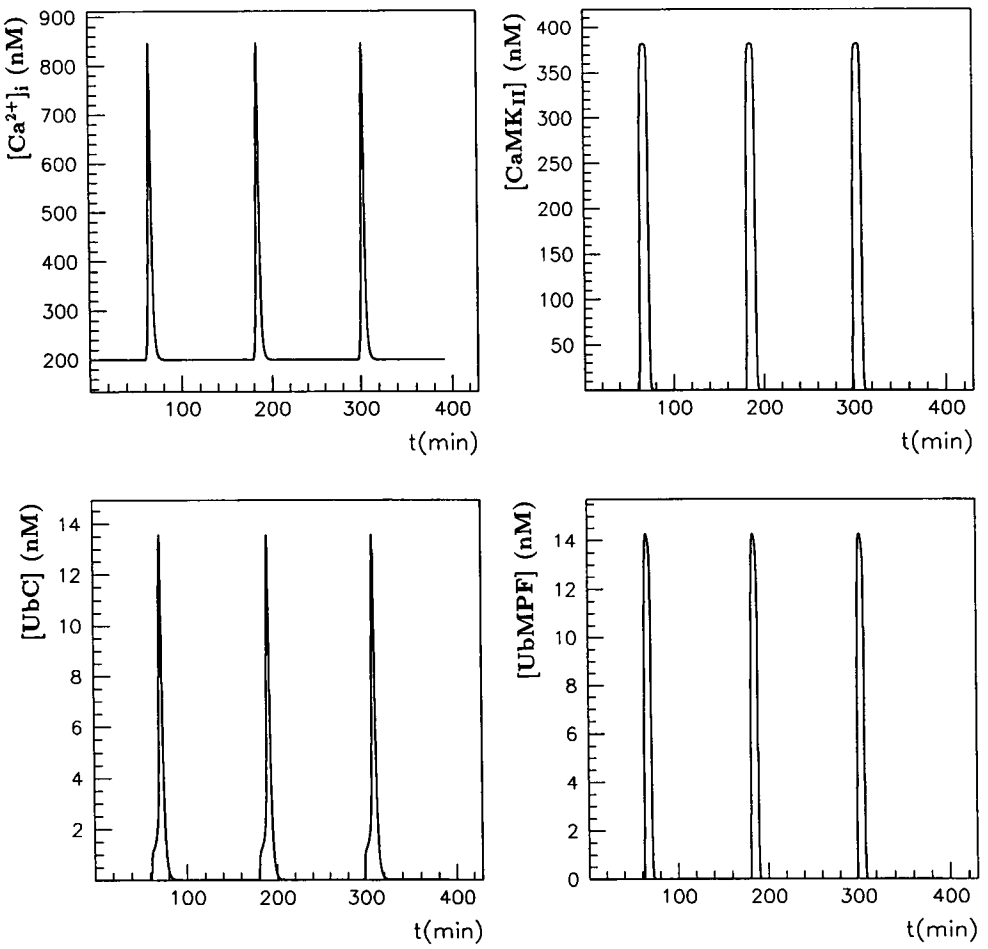

FIGURE 4 The dynamics of cytosolic calcium ($[Ca^{2+}]_i$), $CaMK_{II}$ holoenzyme, ubiquitination complex ([UbC]), and ubiquitinated cyclin B · $p34^{cdc2}$ kinase complex ([UbMPF]) concentrations.

ranges of the kinetic parameters. However, we emphasize the cell specificity of the parameter values, which particularly determines the differences in the cell cycle duration between distinct cell lines. Even within the same cell line the cell cycle time distribution is not uniform, mainly because of the variability of the G_1 phase, as it muchly depends on cell size, cAMP (Baroni et al., 1994; Tokiwa et al., 1994), or external signals. Our model does not include the dependence of cyclin B accumulation on G_1 cyclins. Therefore the G_1 duration is only determined here by the dynamics of the ubiquitination complex and CA.

As suggested (Baran, 1994a, b), anaphase onset is assumed to be determined by a threshold concentration of cytosolic free Ca^{2+}, which is exactly correlated to the maximum [MPF] + [UbMPF] level (Baran, 1994a). The threshold concentration obtained, $[Ca^{2+}]_i^{th} = 238$ nM, is invariable at large variations of the kinetic parameters used. Moreover, it corresponds to the minimum [MPF] + [UbMPF] level (i.e., zero) for the parameters given above. Yet, it is not clear whether Ca^{2+} comes back to the basal level before or after the end of mitosis. However, the system of equations can yield both of these situations with appropriate parameter values. In what follows we shall assume that telophase, not anaphase as previously proposed (Baran, 1994a), ends when [MPF] + [UbMPF] = 0, and we assume a correlation between $[Ca^{2+}]_i^{th}$ and both the maximum and minimum [MPF] + [UbMPF] levels (see Fig. 5). Although it is not clear whether MPF (here MPF and UbMPF) is absent at the end of telophase, we suspect it is, as active MPF induces many protein phosphorylations necessary for nuclear division. They are responsible for the nuclear envelope breakdown by lamin phosphorylation (Murray, 1992) in fission, but not budding, yeast; for chromosome condensation by phosphorylation of histone H_1; and for large changes in cytoskeleton by caldesmon phosphorylation (Yamashiro et al., 1991). In this context we define nuclear division as the period when MPF is active, i.e., [MPF] + [UbMPF] > 0. Nuclear division is followed by cytokinesis, which splits the cell with two nuclei into two mononucleate cells. The end of cell division is formally established here by restoring the basal concentration of Ca^{2+} in cytosol, $[Ca^{2+}]_{i,0}$.

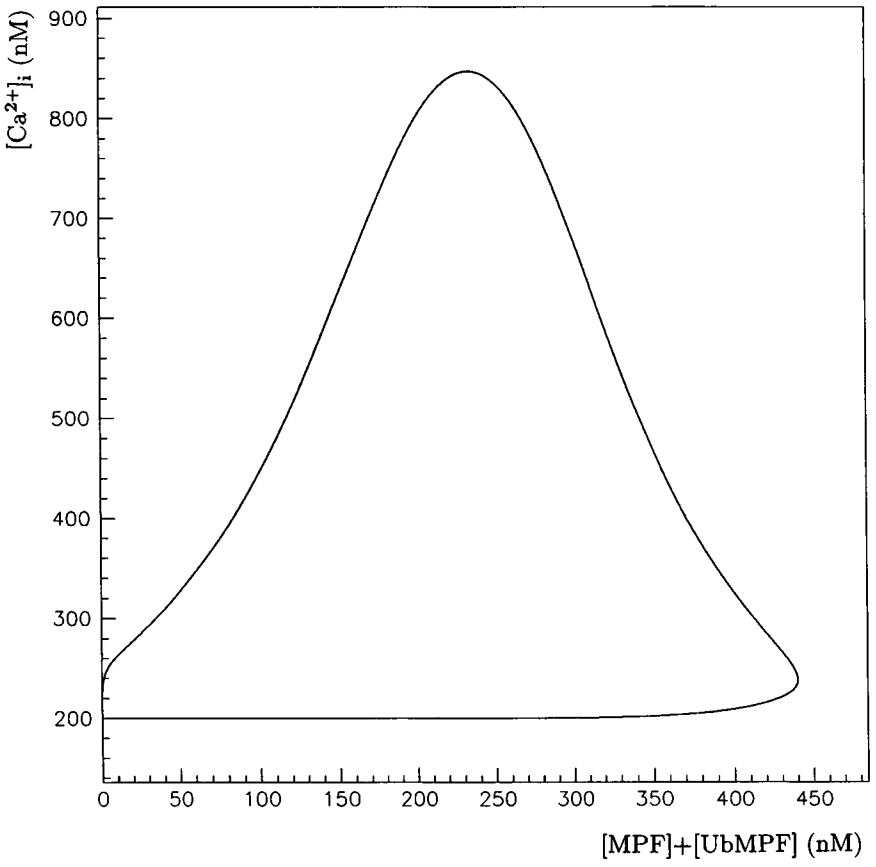

FIGURE 5 Dependence of the cytosolic calcium concentration on the concentration of MPF together with the ubiquitinated complex UbMPF concentration. The threshold value of $[Ca^{2+}]_i$ (238 nM) marks the onset of anaphase ([MPF] + [UbMPF] = maximum) and the end of nuclear division ([MPF] + [UbMPF] = 0), respectively.

In conclusion, the model yields the following quantities:
Beginning of the cell cycle:

t_0 = 0 (0)

Disappearance of Y_{10} and accumulation of Y_1 (it is likely that this moment is placed in S phase):

t_1 = 28 min (0.235)

Mitosis onset:

t_M = 93 min (0.77)

Beginning of anaphase:

t_A = 105 min (0.88)

Beginning of cytokinesis:

t_T = 115 min (0.96)

End of cell division:

t_c = 120 min (1)

where the respective cell cycle time fractions are shown in parentheses.

Indeed, nuclear division is a very short phase (here 22 min) with respect to the cell cycle duration (here 120 min). For instance, John (1981) gave 15 min for the nuclear division period within a 132-min cell cycle time. The values obtained are in agreement with the data of John (1981) and Slater (1977), with one exception: the time spent during cytokinesis, as defined in the model, is very short (here 5 min) as compared to the 24-min value of Slater, or the 31 min given by John. But we have to point out that the numerical values of the moments mentioned above can be varied by modifying the parameter values within appropriate ranges.

MITOSIS STIMULATION/INHIBITION BY *wee1*

The kinetics of the enzymatic process with noncompetitive inhibition considered as in Eq. 1 incorporates the concentration of the inhibitor (the *wee*1 gene product) in the constant K_1 appearing in Eq. 5 (see Appendix). We have then studied the dependence of mitosis on this constant. The results, shown in Fig. 6, suggest that low concentrations of inhibitor (*wee*1 product) may lead to a rapid progression through mitosis by inducing large rises in the calcium concentration. These in turn induce increased levels of the ubiquitination complex, which may affect the next G_1 phase. At lower amplitudes of the calcium transient division is slower, and finally, at high concentrations of inhibitor, mitosis can be blocked, by preventing the calcium rise.

POSSIBLE EFFECTS OF EXTERNAL PERTURBATIONS

With the use of the system of ordinary differential equations proposed in the previous section, it may be possible to characterize several effects of an external field on the cellular level, if the sites and strength of interaction are specified. As long as we can differentiate between the molecular pathways that are affected by this interaction, we may assume that kinetics changes only through its constants and leaves unchanged its functional dependence on the state variables. Therefore the subject under consideration is now

the prediction of the possible mitotic behavior of the cell when considering different combinations of stimulation-sensitive elements in the sequence of mitotic events.

Influence on the extracellular calcium influx

An important influence on calcium metabolism is due to extracellular calcium. In the present situation this feature can be seen by modifying the extracellular influx terms in Eq. 11, which means varying the parameter s_6 and/or the constants that appear either in the IP_3-related term $\alpha([IP_3])$ defined by Eq. 12, or in the influx $\phi([Ca^{2+}]_s)$ induced by the depletion of calcium stores. The change in the sum $s_6 + \phi([Ca^{2+}]_s)$ can be practically followed, for instance, either by changing the concentration of calcium in the extracellular medium or by blocking/opening different IP_3-independent calcium channels on the plasma membrane (through voltage or molecular external signals). In this case the use of a periodic time variation of s_6 or $\phi([Ca^{2+}]_s)$ is particularly justified when an oscillating electric field is applied, as it will be considered later on. There is also the possibility of operating different calcium channels in the plasma membrane by a second messenger (IP_3). This was actually the motivation for introducing the contribution α ($[IP_3]$) in Eq. 11. However, we are not concerned now with the calcium oscillations, usually induced within seconds, that accompany, for example, lymphocyte activation or hepatocyte stimulation. This behavior results exclusively from a specific stimulation of the cell in a characteristic state (lymphocytes are in the resting phase G_0). We cannot consider at the moment the dependence of the calcium signal pathway on other than the mitotic processes, because we suspect that the mitotic status of the cell does not allow the pre-mitotic calcium-specific pathways to be activated in an identical way during mitosis. A similar situation was observed in experiments with T lymphocytes subjected to low-frequency electromagnetic fields, where only activated cells did respond to the external field by modifying their calcium metabolism. However, these aspects are not yet explained and therefore need further investigation.

In this context we have studied the influence of the extracellular calcium influx s_6, assuming that there is a direct relation between the value of s_6 and the activity of pumping Ca^{2+} out of the cell (given by the linear term in Eq. 11). So, we may consider a functional dependence $k_6 = k_6(s_6)$ that helps prevent overaccumulation of Ca^{2+} in cytosol. The choice of this dependence is easily determined by

$$k_6 = \frac{s_6}{[Ca^{2+}]_{i,0}}. \tag{21}$$

The results are depicted in Figs. 7 and 8, indicating a monotone decreasing of the maximum cytosolic Ca^{2+} and ubiquitination complex concentration, respectively. Low $[UbC]_{max}$ concentrations can alter progression through the next G_1. Instead, the pattern of MPF activation-inactivation was not affected by the s_6 value. The weak activity of the calcium pump on the plasma membrane at low s_6 leads to increased Ca^{2+} concentrations. In this case, particularly for $s_6 = 0$, the contribution of the binding term should be considered in Eq. 11, so that the binding term operates only during mitosis.

Periodic external fields

When the cell is subjected to a periodic field that affects intracellular calcium kinetics, we may assume that the calcium fluxes sensitive to this perturbation follow periodically the variation of the field. Hence the characteristic coefficients in Eq. 11 become oscillatory.

The prime calcium currents susceptible to such coupling are the extracellular calcium influxes. The application of an oscillating electric field of the form

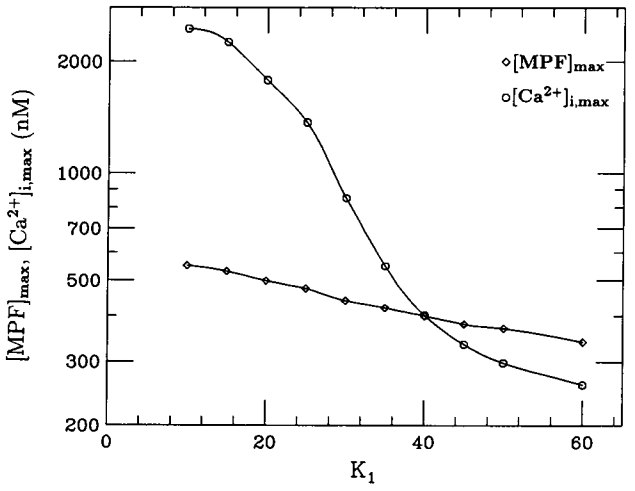

FIGURE 6 Dependence of the amplitude of MPF and cytosolic calcium oscillations on the constant K_1, which increases proportionally with the concentration of the mitosis inhibitor *wee*1 product, according to Eq. 31.

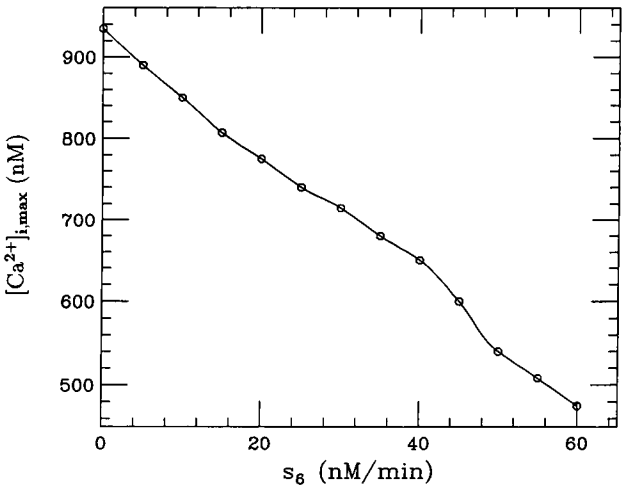

FIGURE 7 The influence of the steady calcium influx through the plasma membrane (s_6) upon the highest cytosolic calcium concentration ($[Ca^{2+}]_{i,max}$) reached in mitosis.

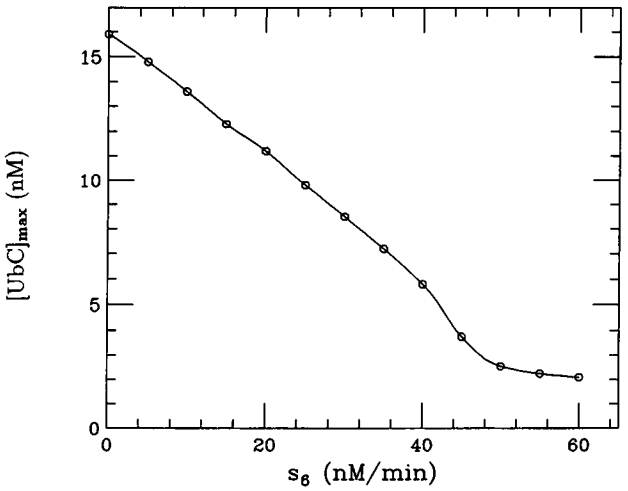

FIGURE 8 The effect of s_6 on the maximum concentration ($[UbC]_{max}$) of the ubiquitination complex.

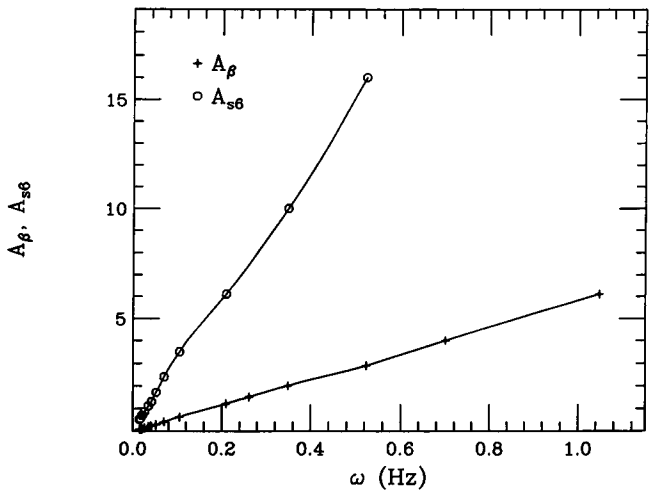

FIGURE 9 Plot of the maximum interaction strength (see explanation in text) that does not perturb cell proliferation, as compared to the control cell cycle oscillations (Figs. 3 and 4), at very low frequency of the oscillating external field.

$$V(t) = V_0 \cos(\omega t) \tag{22}$$

results in the substitution

$$\phi([Ca^{2+}]_s) \rightarrow (1 - A_\phi \sin(\omega t)) \cdot \phi([Ca^{2+}]_s), \tag{23}$$

because the calcium current $\phi([Ca^{2+}]_s)$ is considered to be of the capacitive type. In Eqs. 23 and 24, ω is the frequency of the field, and the modulating amplitude A_ϕ is related to the strength of the specific interaction, which may depend on the cell status and the field intensity.

The mitotic behavior of the cell was found to be most sensitive to the alteration of the activity of pumping Ca^{2+} out of cytosol and, as well, to the perturbation of the passive flux that carries the Ca^{2+} ions out of the intracellular calcium stores. These aspects can be viewed by modifying either the term $\beta([Ca^{2+}]_i)$ or the negative linear terms $-h_6[Ca^{2+}]_i$ and $-h_5[Ca^{2+}]_s$, respectively, in Eqs. 8 and 11. Unlike the noncritical effects on the other terms that contribute to the total calcium flux, it seems that relatively weak actions upon these three terms can easily cause the cell to cease proliferation either by undergoing cell cycle arrest in interphase before activating MPF or, on the contrary, by blocking cellular division without exiting from mitosis.

We have assumed an oscillatory modulation of an oscillating external field to be induced during mitosis, upon the activity of the AMP-driven pump that pumps Ca^{2+} into the stores:

$$\beta([Ca^{2+}]_i) \rightarrow (1 + A_\beta \cos(\omega t))\beta([Ca^{2+}]_i), \tag{24}$$

or, alternatively, upon the inward calcium current s_6,

$$s_6 \rightarrow (1 + A_{s6} \cos(\omega t)) s_6. \tag{25}$$

The maximum A_β at which mitosis is still not perturbed depends on ω, as depicted in Figs. 9 and 10. At a large period (15–20 min) of the external field, the maximum A_β approaches a constant value (0.3). Similar ω dependence is

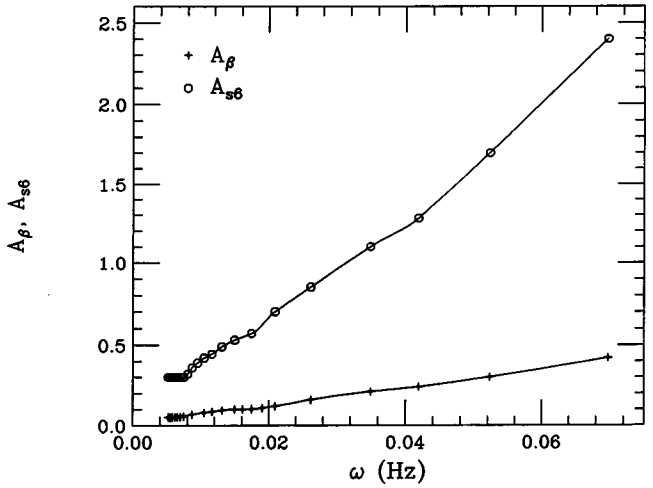

FIGURE 10 The same as in Fig. 9, when increasing the period of the external field.

shown by A_{s6}, as seen in Figs. 9 and 10. The same behavior was obtained for the other calcium pump component ($-k_6[Ca^{2+}]_i$), whereas $\phi([Ca^{2+}]_s)$ affects cell division at very large variations (i.e., high A_ϕ) induced by the oscillatory field as

$$\phi([Ca^{2+}]_s) \rightarrow (1 + A_\phi \cos(\omega t))\phi([Ca^{2+}]_s). \tag{26}$$

Instead, when the IP_3-releasing pathway is affected through the coefficient k_{34} in Eq. 7, completion of mitosis may be successful, but depletion of stores and large increases in cytosolic Ca^{2+} can be induced. They are further reflected in the next G_1 phase because the ubiquitination complex reaches high values and vanishes over a longer time.

Microinjection of Ca^{2+} in cytosol

It is well known that microinjections of calcium in cells blocked near anaphase are able to drive them to interphase (Alberts et al., 1989; McIntosh and Koonce, 1989). We then addressed the question of how the solution of the dynamical system under study behaves when a calcium "impulse" is applied in mitosis. To answer this question, a single instantaneous increase in $[Ca^{2+}]_i$ was applied at different moments during mitosis, and the subsequent evolution of the ten cellular variables was followed.

Three distinct situations have been encountered. First, if calcium microinjection is applied at G_2-M transition (MPF is absent or is at a very low level), then mitosis is completely abolished, because the induced ubiquitination complex rapidly degrades cyclin B and thus prevents MPF accumulation. The question then arises as to whether the ubiquitination complex may be produced before MPF activation. If this is not the case, then a direct relation between MPF level and UbC production should be considered. Furthermore, we should remember here that the feedback mechanism that relates G_1 phase to the completion of the previous mitosis was not included in the model. In this case abolishment of mitosis does not mean transition to the next cell cycle, as the dynamical system admits this solution, but arrest in G_2-M until the conditions for MPF accumulation are met again (i.e., [UbC] decreases to zero). Therefore the system of equations, in its present form, is not applicable to following the influence of calcium microinjection upon cell proliferation, if injection is applied in early mitosis.

Second, if the Ca^{2+} increase is induced when MPF is at significant levels, but before reaching its maximum, the solution of the system yields an incomplete mitosis, as the MPF maximum is greatly reduced, as is the ubiquitination complex level. Not only is the MPF concentration affected, but the duration of the division phase is modified as well.

Third, if the moment of injection is placed in late metaphase–early anaphase, after the moment of maximal activity of MPF, small amounts of injected calcium have relatively weak influence on the mitotic events, because the calcium surplus is quickly pumped out of the cytosol. Instead, at higher amounts of injected calcium, the increase in cytosolic calcium concentration propagates in part to the stores, which then release Ca^{2+} back into the cytosol, and inactivation of MPF is followed by a longer G_1, because [UbC] is increased and vanishes after a longer time. Meanwhile, the delay of G_1 is enhanced by relaxation of calcium stores, which come back to their steady content of calcium. Likewise, in late anaphase–telophase the effect on MPF inactivation is very poor, with visible consequences for the stores' overloading-relaxation regime, and additional ubiquitination complex is produced, which again prolongs G_1. Fig. 11 shows that delaying of the next mitosis is increased as the moment of calcium injection progresses from late metaphase toward the end of mitosis. Concomitantly, a threshold Δ_{ca} value appears to govern the effect in the present situation, and it gradually diminishes as τ_{inj} increases.

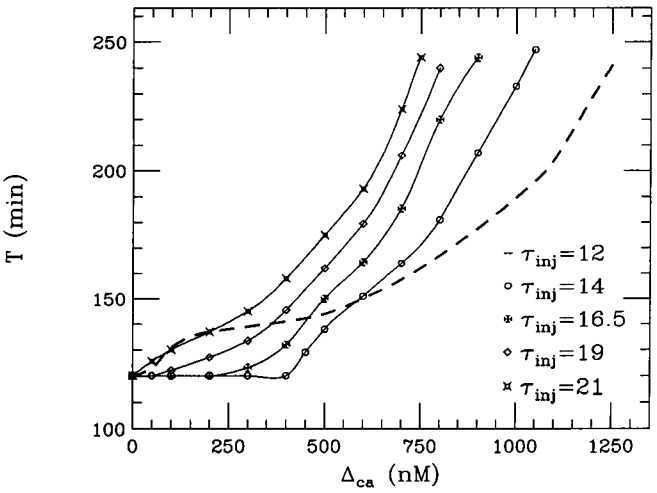

FIGURE 11 Delay of the cell cycle duration induced by microinjections of calcium at different moments, τ_{inj} (min), in mitosis. The time needed for completing the cell cycle after injection (T) is plotted versus the amount of injected Ca^{2+} (Δ_{ca}).

Externally sustained Ca^{2+} influx (ESCI)

If microinjection is very slow or if a calcium influx is induced from the outside over a certain period during mitosis, then an additional constant term (restricted to this interval), denoted I_{ESCI}, in Eq. 11 must be introduced. With this procedure we observed that if I_{ESCI} is applied before the moment of maximum MPF, the resulting increase in cytosolic calcium concentration alters the normal progression of cellular division, because none of the mitotic species (except $[Ca^{2+}]_s$) reaches its normal maximum, and $[Ca^{2+}]_s$, instead of decreasing, rises, so that there is no net release of Ca^{2+} from the stores, but, on the contrary, a part of the cytosolic calcium surplus transiently goes into the stores. Consequently, MPF is inactivated earlier because the inactivation complex appears earlier as well. There may be mechanisms that do not allow the release of calcium before the spindle is readily assembled (and intact) for anaphase. Therefore the forced increase in $[Ca^{2+}]_s$ before anaphase may interfere with the spindle formation. Yet if the spindle is successfully assembled, the low MPF level (which determines the degree of protein phosphorylations in mitosis) does not allow the maximum degree of phosphorylations to be reached in metaphase. This may lead to an improper mitosis and have a lethal effect.

Instead, ESCI applied in anaphase-telophase has effects similar to those of microinjections of calcium (Fig. 12). We have to mention here that, depending on the moment of injection or ESCI, there is a critical value of Δ_{ca} and I_{ESCI}, respectively, that induces the disappearance of the oscillations and maintains the system in a steady state with all parameters practically zero. The common feature of all

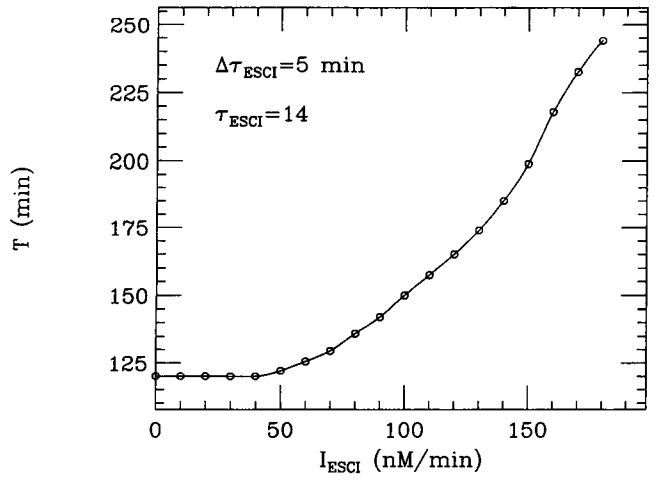

FIGURE 12 The cell cycle period after an externally sustained calcium influx (I_{ESCI}) is induced at the moment τ_{ESCI} in mitosis, over the interval $\Delta\tau_{ESCI}$.

these critical transitions is the maximum value of the oscillations period T, which is determined to be ~249 min.

Depletion of calcium stores

A similar pattern is obtained when a massive release of calcium is induced after the moment of maximum MPF, by introducing a negative term, namely, $-I_{dep}$, on the right side of Eq. 8 and, accordingly, the positive term, I_{dep}, on the right side of Eq. 11. The succession of mitotic events is not affected by the large increase in cytosolic calcium, but onset of cyclin B accumulation is delayed by the ubiquitination complex.

DISCUSSION: HINTS FOR EXPERIMENTS

Our investigations suggest that calcium feeding of cells in mitosis is beneficial when it is targeted at anaphase or telophase, in the case of normal division, or even at late metaphase, if cells are lacking a proper calcium release apparatus. However, the stimulatory effect holds at small amounts of injected calcium, so that division processes are negatively affected when the intensity of ESCI or the amount of injected calcium becomes greater than a threshold value. The threshold value appears to depend on the temporal placement of calcium feeding during the different subphases of mitosis. Even more, the inhibitory influence of large increases in cytosolic free calcium in mitosis may extend to the next G_1-S phases, by indirectly modulating the ubiquitination complex and, implicitly, the cyclin B levels.

Progression through G_1 may be as well altered by applying a periodic field that operates on the IP_3 production pathway. This interaction might be mediated by the G protein pathway (Eichwald and Kaiser, 1993). Strong interactions can lead to depletion of stores and therefore to very high calcium concentration in cytosol.

If confirmed, these predictions might be used in cancer therapy, on the basis of testing the possible role of calcium in inhibiting cellular proliferation.

It seems intriguing that free calcium appears at raised levels in cells at or immediately after the two most important decision points in the cell cycle: Start and anaphase onset. Moreover, calcium is widely known to have a key role in many cellular processes (Berridge, 1993), and the richness of calcium-related responses of cells to external signals shows that calcium is closely connected to the cell status. Cancerous cells also respond to ionizing radiation by increases or oscillations in cytosolic calcium that depend on the phase of the cell cycle. Activated but not resting lymphocytes exhibit calcium oscillations in cytosol when exposed to low-frequency electromagnetic fields (Walleczek and Budinger, cited in Eichwald and Kaiser, 1993).

These observations, taken together with our numerical investigations, led us to the idea that pre-Start G_1 phase might be set up so that the apparatus for calcium release is inactive until Start. The implicit assumption following this consideration is that changes (induced by drugs, for example) in the content of intracellular calcium stores could affect the G_1 duration.

During our study, several problems appeared with regard to the limits of application of the model. Because the model proposed here refers to the normal cell cycle progression, it was clear that its solution obtained when a perturbation is applied can be realistic as long as the perturbation does not activate mechanisms in the cell that are not included in the equations.

The most striking difficulties have been encountered when MPF accumulation was inhibited during mitosis, because without the restriction that prevents cell commitment (at Start) to the next division if the previous mitosis is not complete, the system of equations cannot yield a realistic effect of the external perturbation upon cellular dynamics. This situation was met when the moment of perturbation was chosen in early mitosis. In this case we address the following questions:

i) *May calcium be released from internal stores before the end of spindle assembly?* The answer is likely to be negative, because the impressive flexibility of living cells in their response to many perturbations is based on a net of control mechanisms that are only then activated when needed. Hence, if spindle formation is blocked, there must be mechanisms activated to prevent anaphase onset. Otherwise, the cell divides improperly and eventually dies.

ii) *Does a direct MPF control operate on the calcium-calmodulin pathway of production of the ubiquitination complex?* If this control is absent, mitosis might be easily blocked or abolished if a calcium increase in cytosol is induced in early mitosis.

iii) *Can calcium be released during G_1?* This point refers to the possibility of inducing Ca^{2+} oscillations in activated, but not resting, lymphocytes. Consequently,

iv) *Is there a correlation between the content of intracellular calcium stores and progression through G_1 phase?* If

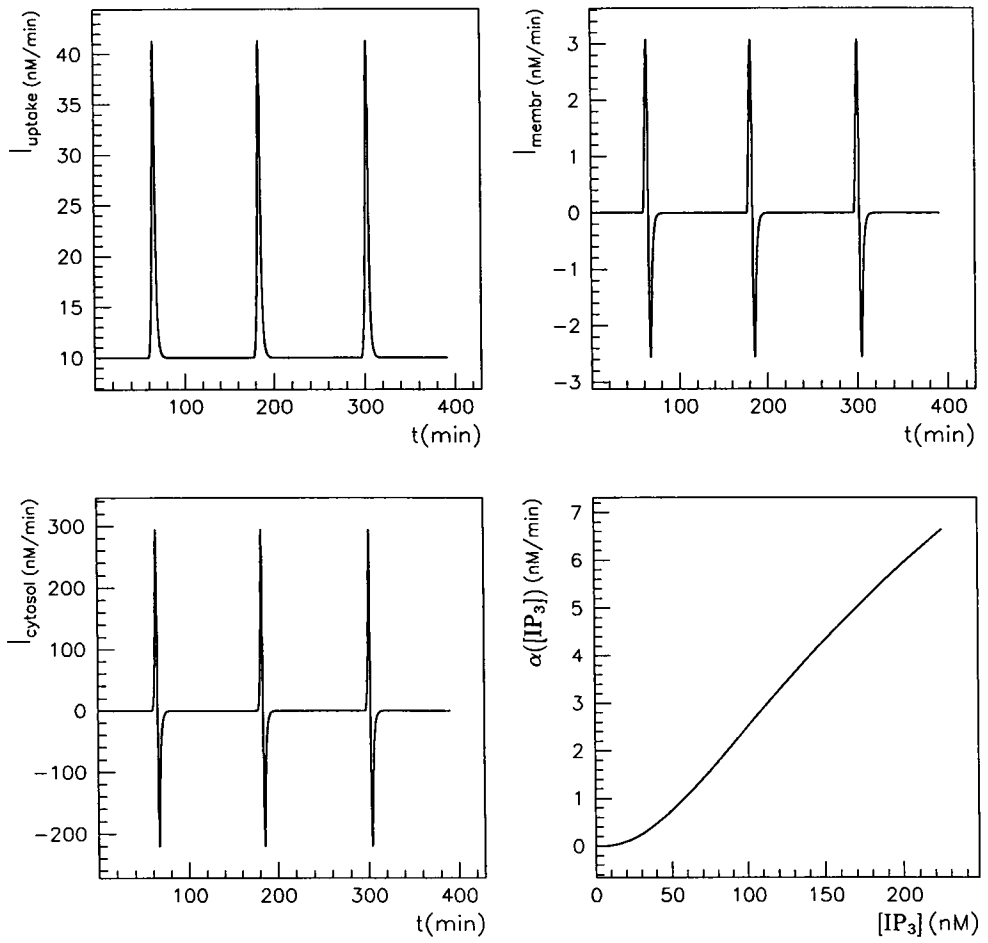

FIGURE 13 Calcium dynamics reflected in the different cellular calcium flows. In the lower right the dependence of the IP_3-related calcium influx ($\alpha([IP_3])$) on the IP_3 concentration is depicted.

"yes," then alteration of stores content might cause the cell to cease proliferation by arrest in G_1.

v) *Are the mechanisms that lead to calcium oscillations in stimulated cells active in mitosis?* In other words, can an external stimulus have an effect on the IP_3-induced calcium release in mitosis similar to that in interphase? As we discussed before, a periodic variation in the rate of IP_3 production during mitosis might inhibit cellular proliferation.

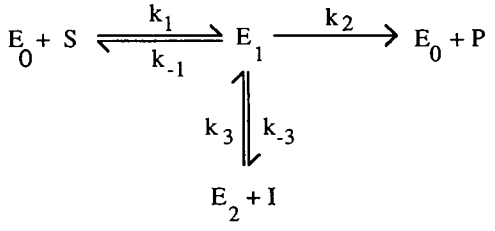

FIGURE 14 An enzymatic process with noncompetitive inhibition. The quantities on the arrows represent the first-order rate constants, and I signifies the inhibitor.

Beyond these unclarified aspects, several predictions of the present model can be tested in experiments, as presented in the previous sections, particularly with the use of calcium measurements.

Thus, if the dynamics of free cytosolic calcium is monitored during G_2 mitosis progression (by fluorescent marker techniques, for example) as a function $[Ca^{2+}]_i(t)$, then the cytosolic calcium current, defined as

$$I_{\text{cytosol}} = \frac{d[Ca^{2+}]_i(t)}{dt}, \tag{27}$$

is accessed by simple derivation with respect to time. A simultaneous determination of the total calcium flow through the plasma membrane fitted by

$$I_{\text{membr}} = \alpha([IP_3]) + \phi([Ca^{2+}]_s) + s_6 - k_6 \cdot [Ca^{2+}]_i \tag{28}$$

then allows the derivation of the balance of the intracellular (i.e., the exchange between cytosol and stores) and extracellular calcium flows at different moments as

$$I_{\text{store}} = I_{\text{cytosol}} - I_{\text{membr}}, \tag{29}$$

where

$$I_{store} = -\frac{d[Ca^{2+}]_s(t)}{dt}. \quad (30)$$

In summary, having access to $[Ca^{2+}]_i(t)$ and $I_{membr}(t)$, the content of calcium stores can be obtained by integrating Eq. 30.

Additional information could be obtained if a distinction between different components (see Eq. 11) of the calcium flow through the plasma membrane were made. In this sense, the steady current s_6 can be determined by measuring the calcium uptake from the extracellular medium during a cell phase with a steady cytosolic Ca^{2+} concentration. In this way the values of s_6 and k_6 are obtained. Furthermore, if the calcium exchange with the extracellular medium is determined during mitosis, then the IP_3- and $[Ca^{2+}]_s$-related calcium incoming current, $\alpha([IP_3]) + \phi([Ca^{2+}]_s)$, can be easily derived by the corespondent difference. A further distinction between $\alpha([IP_3])$ and $\phi([Ca^{2+}]_s)$ would allow us to obtain the parameters k_{64}, q, and K_M in Eq. 12 (by fitting the curve obtained as in Fig. 13) and ϕ_0 and ϕ_1 in Eq. 13 as well.

In addition, for a very large variation of the constant parameters used in the equations, we obtained a linear dependence of cytosolic Ca^{2+} concentration and the content of the calcium stores. For this reason, it is likely that the dimension of the system may be reduced to nine.

In conclusion, we propose a model for studying the possible role of calcium in mitosis and cell proliferation, based on knowledge of the main molecular events that lead to cell division. Several emerging predictions can be tested in experiments. The model is open to improvements that may include other cell cycle control mechanisms, so that it could be further connected with a more realistic description of progression through G_1 and S phases. Further investigations are still needed to unveil the molecular steps involved in cell cycle progression that are not yet clarified or even known. Then, with realistic and performent models, cellular kinetics can be followed in large cell populations, aiming at efficient programs to be used in different therapeutic procedures.

APPENDIX

The enzymatic processes with noncompetitive inhibition consist of the reactions depicted in Fig. 14 (Volkenshtein, 1983). In this case the equivalent Michaelis-Menten equation takes the form

$$-\frac{dS}{dt} = \frac{dP}{dt} = \frac{k \cdot S}{K_M + K \cdot S} \quad (31)$$

where $K_M = (k_2 + k_{-1})/k_1$, $K_I = k_3/k_{-3}$, $k = k_2E$, $K = 1 + K_II$, $E = E_0 + E_1 + E_2$ and I, E = const.

In the paper this form is used with other names for the parameters. Applying Eq. 31 in the particular case when CB and pre MPF are the substrate and, respectively, the product in a similar process, the term $k_1[CB]/(K_{1M} + K_1[CB])$ is then used in Eqs. 4 and 5.

REFERENCES

Alberts, B., D. Bray, J. Lewis, M. Raff, K. Roberts, and J. D. Watson. 1989. Molecular Biology of the Cell, 2nd ed. Garland Press, New York.

Amon, A., S. Irniger, and K. Nasmyth. 1994. Closing the cell cycle circle in yeast: G2 cyclin proteolysis initiated at mitosis persists until the activation of G1 cyclins in the next cycle. *Cell.* 77:1037–1050.

Baran, I. 1994a. Exit from mitosis induced by a calcium transient: the relation to the MPF and $InsP_3$ dynamics. *BioSystems.* 33:203–214.

Baran, I. 1994b. Mitosis dependence on cytosolic Ca^{2+} in relation to the cell cycle progression. *In* Charge and Electric Fields Effects in Biosystems 4. M. J. Allen, S. F. Cleary, and A. E. Sowers, editors. World Scientific Publishing, Singapore. 3–11.

Baroni, M. D., P. Monti, and L. Albergina. 1994. Repression of growth-regulated G_1 cyclin expression by cyclic AMP in budding yeast. *Nature.* 371:339–342.

Berridge, M. J. 1993. Inositol triphosphate and calcium signalling. *Nature.* 361:315–325.

Camacho, P., and J. D. Lechleiter. 1993. Increased frequency of calcium waves in *Xenopus laevis* oocytes that express a calcium-ATPase. *Science.* 260:226–229.

Chay, T. R. 1993. Modelling of nonlinear dynamical processes in biology. *In* Patterns, Information and Chaos in Neuronal Systems. B. J. West, editor. World Scientific Publishing, River Edge, NJ. 74–122.

Clapa, B., D. Pesando, M. Wilding, and M. Whitaker. 1994. Cell-cycle calcium transients driven by cyclic changes in inositol triphosphate levels. *Nature.* 368:875–878.

Dubois, J.-M., and B. Rouzaire-Dubois. 1993. Role of potassium channels in mitogenesis. *Prog. Biophys. Mol. Biol.* 59:1–21.

Eichwald, C., and F. Kaiser. 1993. Model for receptor-controlled cytosolic calcium oscillations and for external influences on the signal pathways. *Biophys. J.* 65:2047–2058.

Elledge, S. J., R. Richman, F. L. Hall, R. T. Williams, N. Lodgson, and J. W. Harper. 1992. CDK2 encodes a 33-kDa cyclin A-associated protein kinase and is expressed before CDC2 in the cell cycle. *Proc. Natl. Acad. Sci. USA.* 89:2907–2911.

Félix, M.-A., J.-C. Labbé, M. Dorée, T. Hunt, and E. Karsenti. 1992. Triggering of cyclin degradation in interphase extract of amphibian eggs by *cdc2* kinase. *Nature.* 346:379–382.

Finch, E. A., T. J. Turner, and S. M. Goldin. 1991. Calcium as coagonist of inositol 1,4,5-triphosphate-induced calcium release. *Science.* 252: 443–446.

Glotzer, M., A. W. Murray, and M. W. Kirschner. 1991. Cyclin is degraded by the ubiquitin pathway. *Nature.* 349:132–138.

Gould, K. L., and P. Nurse. 1989. Tyrosine phosphorylation of the fission yeast cdc^{2+} protein kinase regulates entry into mitosis. *Nature.* 342: 39–45.

Hartwell, L. H. 1974. *Saccharomyces cerevisiae* cell cycle. *Bacteriol. Rev.* 38:164–198.

Hartwell, L. H., and T. A. Weinert. 1989. Checkpoints: controls that ensure the order of cell cycle events. *Science.* 246:629–634.

Hoth, M., and R. Penner. 1992. Depletion of intracellular calcium stores activates a calcium current in mast cells. *Nature.* 355:353–356.

Hunt, T. 1992. Under arrest in the cell cycle. *Nature.* 342:483–484.

Iino, M., and M. Endo. 1992. Calcium-dependent immediate feedback control of inositol 1,4,5-triphosphate-induced Ca^{2+} release. *Nature.* 360: 76–78.

John, P. C. 1981. The Cell Cycle. Cambridge University Press, Cambridge.

Kasai, H., Y. X. Li, and Y. Miyashita. 1993. Subcellular distribution of Ca^{2+} release channels underlying Ca^{2+} waves and oscillations in exocrine pancreas. *Cell.* 74:669–677.

Knoblich, J. A., K. Sauer, L. Jones, H. Richardson, R. Saint, and C. F. Lehner. 1994. Cyclin E controls S phase progression and its down-regulation during Drosophila embyogenesis is required for the arrest of cell proliferation. *Cell.* 77:107–120.

Kobayashi, H., E. Stewart, R. Y. C. Poon, and T. Hunt. 1994. Cyclin A and cyclin B dissociate from $p34^{cdc2}$ with half-times of 4 and 15 h, respectively, regardless of the phase of the cell cycle. *J. Biol. Chem.* 269: 29153–29160.

Li, X., and B. Nicklas. 1995. Mitotic forces control a cell-cycle checkpoint. *Nature*. 373:630–632.

Lorca, T., F. H. Cruzalegui, D. Fesquet, J.-C. Cavadore, J. Méry, A. Means, and M. Dorée. 1993. Calmodulin-dependent protein kinase II mediates inactivation of MPF and CSF upon fertilization of *Xenopus* eggs. *Nature*. 366:270–273.

Lückhoff, A., and D. E. Clapham. 1992. Inositol 1,3,4,5-tetrakisphosphate activates an endothelial Ca^{2+}-permeable channel. *Nature*. 355:356–358.

McIntosh, J. R., and M. P. Koonce. 1989. Mitosis. *Science*. 246:622–628.

Mitchison, J. M. 1989. Cell cycle growth and periodicities. *In* Molecular Biology of the Fission Yeast. A. Nasim, P. Young, and B. F. Johnson, editors. Academic Press, New York. 205–242.

Miyazaki, S., M. Yuzaki, K. Nakada, H. Shirakawa, S. Nakanishi, S. Nakade, and K. Mikoshiba. 1992. Block of Ca^{2+} wave and Ca^{2+} oscillation by antibody to the insitol 1,4,5-triphosphate receptor in fertilized hamster eggs. *Science*. 257:251–255.

Moreno, S., and P. Nurse. 1994. Regulation of progression through the G_1 phase of the cell cycle by the *rum1*$^+$ gene. *Nature*. 367:236–242.

Murray, A. W. 1992. Creative blocks: cell cycle checkpoints and feedback control. *Nature*. 359:599–604.

Murray, A. W. 1995. Tense spindles can relax. *Nature*. 373:560–561.

Murray, A. W., and M. W. Kirschner. 1989. Dominoes and clocks: the union of two views of the cell cycle. *Science*. 246:614–621.

Murray, A. W., and M. W. Kirschner. 1991. What controls the cell cycle. *Sci. Am.* March:34–41.

Norel, R., and Z. Agur. 1991. A model for the adjustement of the mitotic clock by cyclin and MPF levels. *Science*. 251:1076–1078.

Novak, B., and J. J. Tyson. 1993. Modeling the cell division cycle: M-phase trigger, oscillations and size control. *J. Theor. Biol.* 165: 101–134.

Novak, B., and J. J. Tyson. 1995. Quantitative analysis of a molecular model of mitotic control in fission yeast. *J. Theor. Biol.* 173:283–305.

Nurse, P. 1990. Universal control mechanism regulating onset of M-phase. *Nature*. 344:503–508.

O'Farrell, P. H., B. A. Edgar, D. Lakich, and C. H. Lehner. 1989. Directing cell division during development. *Science*. 246:635–640.

Ohtsubo, M., and J. M. Roberts. 1993. Cyclin-dependent regulation of G_1 in mammalian fibroblasts. *Nature*. 259:1908–1912.

Pardee, A. B. 1989. G_1 events and regulation of cell proliferation. *Science*. 246:603–608.

Parekh, A. B., H. Terlau, and W. Stühmer. 1993. Depletion of $InsP_3$ stores activates a Ca^{2+} and K^+ current by means of a phosphatase and a diffusible messenger. *Nature*. 364:814–818.

Parker, L. A., and H. Piwnica-Worms. 1992. Inactivation of the $p34^{cdc2}$-cyclin B kinase by the human WEE1 tyrosine kinase. *Science*. 257: 1955–1957.

Randriamampita, C., and R. Y. Tsien. 1993. Emptying of intracellular Ca^{2+} stores releases a novel small messenger that stimulates Ca^{2+} influx. *Nature*. 364:809–814.

Rosenblatt, J., Y. Gu, and D. O. Morgan. 1992. Human cyclin-dependent kinase 2 is activated during the S and G_2 phases of the cell cycle and associates with cyclin A. *Proc. Natl. Acad. Sci. USA*. 89:2824–2828.

Seufert, W., B. Futcher, and S. Jentsch. 1995. Role of a ubiquitin- conjugating enzyme in degradation of S- and M-phase cyclins. *Nature*. 373: 78–81.

Slater, J. H. 1977. Cell cycle of *Saccharomyces cerevisiae* in populations growing at different rates. *Proc. Natl. Acad. Sci. USA*. 74:3850–3854.

Thorn, P., A. M. Lawrie, P. M. Smith, D. V. Gallacher, and O. H. Petersen. 1993. Local and global cytosolic Ca^{2+} oscillations in exocrine cells evoked by agonists and inositol triphosphate. *Cell*. 74:661–668.

Thron, C. D. 1991. Mathematical analysis of a model of the mitotic clock. *Science*. 254:122–123.

Thron, C. D. 1994. Theoretical dynamics of the cyclin B-MPF system: a possible role for $p13^{suc1}$. *BioSystems*. 32:97–109.

Tokiwa, G., M. Tyers, T. Volpe, and B. Futcher. 1994. Inhibition of G_1 cyclin activity by the Ras/cAMP pathway in yeast. *Nature*. 371: 342–345.

Volkenshtein, M. V. 1983. Biophysics. Mir Publishers, Moscow. 193–197.

Walker, D. H., and J. L. Maller. 1991. Role for cyclin A in the dependence of mitosis on completion of DNA replication. *Nature*. 354:314–317.

Walleczek, J., and T. F. Budinger. 1992. Pulsed magnetic field effects on calcium signalling in lymphocytes: dependence on cell status and field intensity. *FEBS Lett.* 314:351–355.

Whitaker, M. 1993. Sharper than a needle. *Nature*. 366:211–212.

Wu, L., and P. Russell. 1993. Nim1 kinase promotes mitosis by inactivating Wee1 tyrosine kinase. *Nature*. 363:738–741.

Yamashiro, S., Y. Yamakita, H. Hosoya, and F. Matsumura. 1991. Phosphorylation of non-muscle caldesmon by $p34^{cdc2}$ kinase during mitosis. *Nature*. 394:169–172.